Journal of Materials Chemistry C

Accepted Manuscript

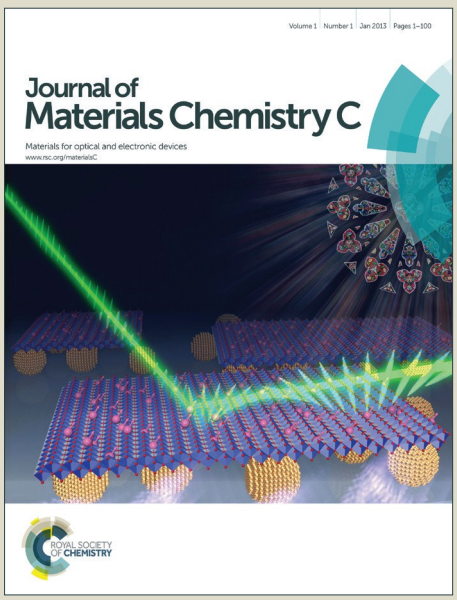

ROYAL SOCIETY OF CHEMISTRY

www.rsc.org/materialsC

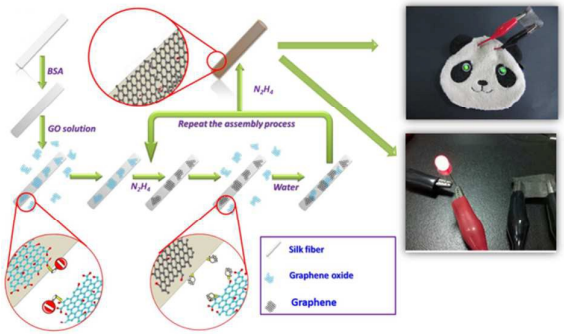

A repeated coating-reduction approach was developed to directly immobilize graphene nanosheets on silk for high conductivity. The as-prepared highly conductive graphene-coated silk fabrics (1.5 kΩ/sq) and fibers (3595 S/m) are promising as the functional supporting matrix and conducting fabrics/wires in future wearable electronics.

Cite this: DOI: 10.1039/c0xx00000x

www.rsc.org/xxxxxx

ARTICLE TYPE

Highly Conductive Graphene-coated Silk Fabricated via a Repeated Coating-Reduction Approach

Zhisong Lu,* [a,b,c] Cuiping Mao,[a,b,c] and Huihui Zhang[a,b,c]

Received (in XXX, XXX) Xth XXXXXXXXX 20XX, Accepted Xth XXXXXXXXX 20XX

DOI: 10.1039/b000000x

A repeated coating-reduction approach was developed to directly immobilize graphene nanosheets on silk for high conductivity. The as-prepared highly conductive graphene-coated silk fabrics (1.5 kΩ/sq) and fibers (3595 S/m) are promising as the functional supporting matrix and conducting fabrics/wires in future wearable electronics.

With rapid advances of miniaturization and wireless technologies, electronics has been associated with traditional textiles to develop smart wearable devices for daily health monitoring and fitness tracking[1, 2]. Silk from *Bombyx mori* cocoons, a natural protein fiber consisting of 18 amino acids, is considered as an ideal support for wearable electronics because of its softness, high hygroscopicity and superior skin affinity[3-6], which fulfill the basic requirements of wearable devices on comfort and flexibility. However, practical applications of silk as building components of wearable devices are still rare due to its lack of specific functions such as sensing and conductivity.

Conductive fibers and fabrics are essential for wearable devices since they may be utilized as components of sensors and pathways for electrical signal transfer. Thus, great efforts have been dedicated to fabricate highly conductive silk-based textile materials for wearable electronics in recent years[7, 8]. Because natural silk can be degraded into silk fibroin proteins *in vitro*, electrically conductive materials such as polypyrrole[9-11], gold nanoparticles[12], gold nanowires[13], single-walled carbon nanotubes[14] and graphene[5] have been composed with fibroin to produce electro-conductive composites. Using this strategy, highly conductive fibroin-based composites with desired morphology could be easily obtained, but a loss in the excellent mechanical property and superior elasticity of the natural silk cannot be avoided. Direct deposition of conductive elements on the fiber/fabric surface is considered to be an alternative method to maintain the silk features. Conducting polymers including poly(3,4-ethylenedioxythiophene): poly(styrenesulfonate) (PEDOT:PSS) as well as polypyrrole and its derives[15] were *in situ* polymerized on silk fabrics to achieve high conductivity. However, the conductivity of the polymers could be affected by oxidant concentration, degree of doping, environmental pH and polymerization time. Moreover, aggregation of the polymers often occurs in the polymerization procedure, resulting in the non-uniform coating. Iridium nanoparticles are also sputtered on silk to obtain flexible conductive microwires[16]. However, the non-uniform coating of iridium nanocrystals and easy crack of iridium layer during stretch significantly hinder the application of the microwires.

Graphene is a one-carbon-atom layer nanomaterial with two-dimensional (2D) morphology, which possesses ultrahigh electron mobility, great thermal conductivity and strong mechanical strength[17]. The potential of graphene in preparation of conductive textiles is demonstrated in a very recent work, in which graphene-silk fiber composites with extremely high conductivity were fabricated by vacuum filtration[5]. Silk fibers are randomly distributed in the composited film, forming a loose network structure. In comparison to the woven fabrics with well-organized structures, the elasticity of the composite film is quite poor. In addition, the structure cannot match the well-established woven techniques either. Thus, it is of great demand to develop an approach for the fabrication of highly conductive graphene coated-silk fabrics without disturbing their well-organized structure. Herein we develop a repeated coating-reduction approach to directly immobilizing graphene nanosheets on woven silk fabrics for high electron conductivity.

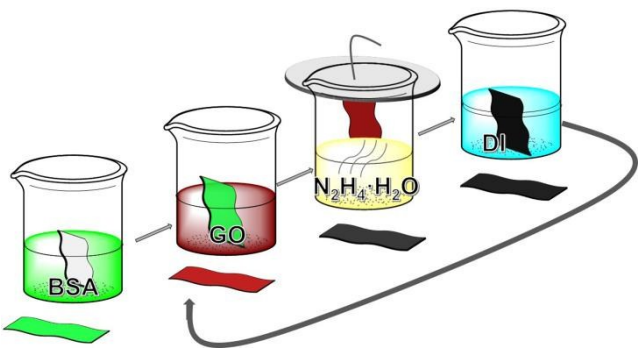

Scheme 1 Preparation of a graphene-coated silk fabric

The quality of freshly prepared graphene oxide (GO) nanosheets was verified with X-ray diffractometry (XRD) and atomic force microscopy (Fig. S1 and S2). Experimental procedures for the preparation of graphene-coated silk are illustrated in Scheme 1. Firstly, bovine serum albumin (BSA), which serves as a universal adhesive to facilitate the adsorption of GO nanosheets[18], is immobilized via hydrophobic adsorption to introduce positive charges on a silk fabric. Then the BSA-functionalized silk fabric is immersed into a GO solution to allow the self-assembly of negatively charged GO nanosheets on silk surface, followed by a hydrazine vapor reduction. After washing

with deionized (DI) water to remove loosely attached graphene nanosheets, the silk with 1st round of graphene coating is obtained. During the coating-reduction process, the color of silk fabric changes from white to brown, finally black (Fig. S3), reflecting the adsorption and the reduction of GO. By repeating the above mentioned coating-reduction procedure, samples with different number of coating cycles are produced. The constructed composite is denoted as $(graphene)_n$/silk, where n is the number of coating-reduction cycles. Since BSA is easily to be denatured, BSA-functionalized silk fabrics were fabricated with a freshly prepared BSA solution and immediately used to adsorb GO after washing. During the coating-reduction cycles, BSA denaturation may be unavoidable. But it is found that the performance of $(graphene)_7$/silk can be maintained for more than 1 month without a significant decrease. The adsorption property of denatured BSA to GO nanosheets is still under investigation in our laboratory.

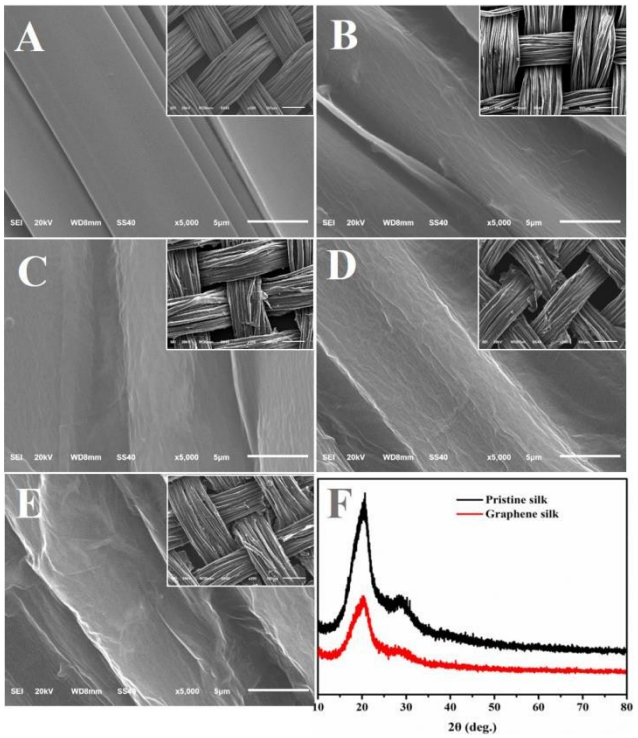

Fig. 1 SEM images of pristine silk fabric (A) and graphene-coated silk fabrics with 1 (B), 3 (C), 5 (D) and 7 (E) rounds of coating-reduction process. Insets are the corresponding SEM images with a low magnification. (F) XRD patterns of pristine silk and graphene-coated silk.

Surface morphologies of the silk fabrics with or without graphene coating were investigated using scanning electron microscopy (SEM) (Fig. 1). The pristine silk fabric shows a well-organized woven structure, which consists of silk fibers with a very smooth surface and an average diameter of ~9 μm. After 1 round of coating-reduction, a wrinkled film can be observed on the surface, suggesting the immobilization of graphene. As the coating-reduction cycle number increases from 3 to 7, more wrinkles appear on the fiber surface and the overlap of nanosheets becomes more obvious. The results indicate that more graphene nanosheets could be immobilized on the silk fabric by repeating the coating-reduction procedure. As being shown in Fig. 1C, 1D and 1E, the graphene films could cover two neighbored silk fibers to form connecting bridges, which may greatly facilitate the electron transfer on the graphene-coated silk fabrics. The side-view SEM images of the graphene-coated silk fabrics show that the modified graphene nanosheets do not break off from the silk surface during the 7 rounds of coating-reduction (Fig. S4). During the modification process, there is no significant alteration on the woven structure as well as silk II and silk I XRD peaks (Fig. 1F). Mechanical properties of the silk fabrics were investigated with the stress-strain curve analysis (Fig. S5). Both tensile strength (~36.91 MPa) and failure strain (~17.88%) of the pristine silk fabrics are larger than those of the graphene-modified ones. However, the elastic modulus of the graphene-coated ones is larger. The data indicate that the coating-reduction procedures may possibly affect the mechanical strength of the silk.

To further verify the efficient reduction of GO, Raman spectra of the modified silk fabrics were collected after each coating and reduction step (Fig. 2). The Raman spectra are weak and noisy because a very small amount of GO or reduced GO is immobilized on the silk fabrics. All samples exhibit two prominent peaks at 1342 and 1577 cm^{-1}, which can be attributed to the D and G bands, respectively. The G band is characteristic for sp^2-hybridized C-C bonds in a two-dimensional hexagonal lattice, while the D band corresponds to the defects and disorder in the planar carbon network[19]. The presence of both D and G bands strongly prove the immobilization of GO sheets on silk fabrics, agreeing well with the SEM images. Since the intensity ratio of D to G band (I_D/I_G) is usually used to evaluate the reduction of GO to graphene, it is plotted against each GO coating and chemical reduction step to illustrate the change of surface properties (Fig. 2B). Interestingly, a sawtooth-shaped curve with lower ratios for GO coating steps and higher ratios for hydrazine reduction steps is observed from the 1st to the 5th coating-reduction cycles. The enhancement of the I_D/I_G ratio after each reduction step proves the successful reduction of GO into graphene. The decline of the ratio after each coating step indicates the introduction of more defects and disorders to samples, further evidencing the efficient adsorption of GO nanosheets on the fabrics. It is also found that the intensity ratio does not significantly change after 5 rounds of coating-reduction. It may indicate that reduced GO nanosheets are prominent on the silk surface and the additional adsorption of GO could not significantly alter the surface properties.

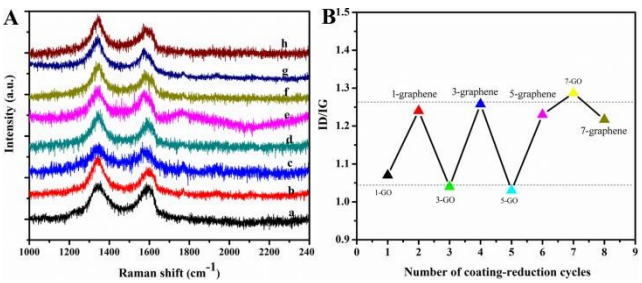

Fig. 2 (A) Raman spectra of the functionalized silk fabrics after each coating and reduction step. The (a), (c), (e) and (g) curves correspond to the fabrics after 1st, 3th, 5th and 7th GO coating, respectively. The (b), (d), (f) and (h) curves correspond to the fabrics after 1st, 3th, 5th and 7th reduction step, respectively. (B) The change of I_D/I_G ratio after each coating and reduction step.

Because the reduction of GO leads to the removal of hydrophilic groups such as hydroxyl and carbonyl groups from the nanosheets, the hydrophilicity of the functionalized silk fabrics may be altered. Originally, the silk fabric after one time of GO coating possesses a hydrophilic surface. However, after 7 rounds of repeated coating-reduction, it changes to a very hydrophobic one with a contact angle of 115° (Fig. S6). Each reduction step results in a significant increment of the water contact angle, also showing the effective reduction of GO. We did Fourier transform infrared spectroscopy (FTIR) to further explore the change of the surface chemical groups on the fabrics (Fig. S7). The GO adsorption could not cause obvious change on the peak patterns (Data not shown) since the chemical groups on GO nanosheets also exist on BSA-immobilized silk fabrics. However, the intensities of all characteristic peaks of BSA-silk fabrics gradually reduce with the increase of the repeating number. The coated graphene nanosheets may block the chemical groups on the silk fibers, thus causing the decrease of peak intensity in FTIR spectra.

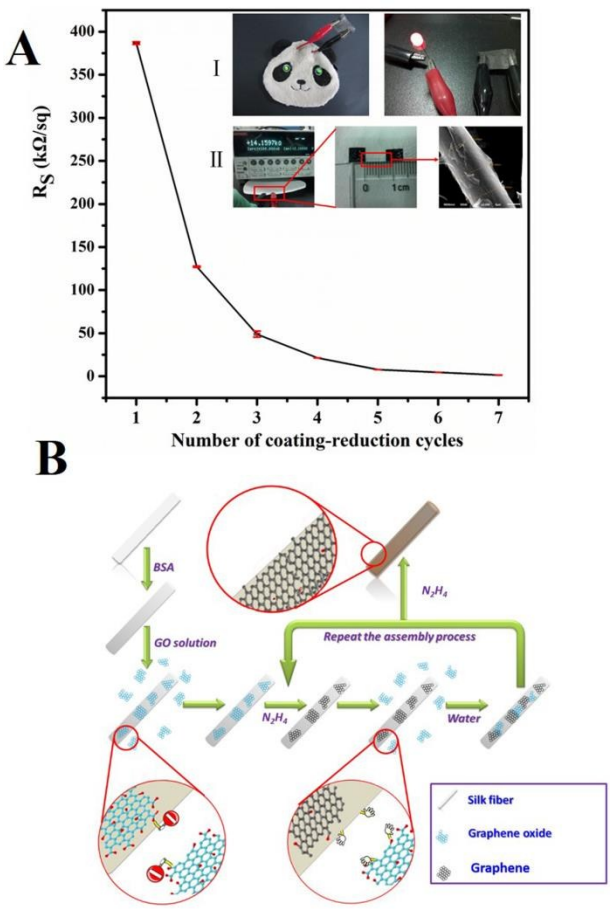

Fig. 3 (A) Effect of coating-reduction cycle on sheet resistance of graphene-coated silk fabrics. Inset I shows a LED light integrated with a graphene-coated silk fabric; Inset II shows a single graphene-coated silk fiber. (B) Mechanism for the efficient graphene nanosheets immobilization.

The sheet resistance (R_s) was measured to show the electro-conductive capability of the $(graphene)_n$/silk fabrics (Fig. 3). As the number of coating-reduction cycle increases, R_s of the modified fabrics continuously declines. The R_s of the original fabrics without coating cannot be detected. The first round of graphene coating makes the fabrics conductive and the value greatly decreases to 386.6 kΩ/sq. Significant improvements of the *Rs* can be observed after 2, 3, 4 and 5 rounds of coating-reduction, respectively. The R_s can reach to 1.5 kΩ/sq for $(graphene)_7$/silk fabrics, which can meet the electron conductive requirement of wearable electronics. Inset I of Fig. 3A illustrates that a $(graphene)_7$/silk fabric could be used as an electrical conductor to light the LED lamps. Since bending and twisting cannot be avoided for wearable devices, effects of bending and twisting on the *Rs* of graphene-silk fabrics were studied. It is found that the R_s of the graphene-silk fabrics keeps stable during 500 times of twisting and bending (Fig. S8), showing the excellent flexibility of the conductive silk fabrics. To demonstrate the adaptability of the approach for fiber functionalization, graphene nanosheets were immobilized on a single silk fiber in the present work. The electrical conductivity of a single $(graphene)_7$/silk fiber is 3595 S/m, which is two order of magnitude higher than those of the reported graphene-coated silk fiber (57.9 S/m)[5], PEDOT-PSS silk thread (10.2 S/m)[15] and polypyrrole-silk fibroin composite fiber (42 S/m)[20].

Undoubtedly, the high conductivity of the modified silk can be attributed to the efficient immobilization of graphene nanosheets. GO solutions with a pH value of 4.0 were utilized in the coating steps. Zeta-potentials of BSA molecules and GO nanosheets at pH 4.0 are 8.90±0.19 mV and -37.97±1.52 mV, respectively, confirming the negative charges of GO and positive charges of BSA during the coating process. Based on the experimental data we propose a mechanism to simulate the graphene nanosheet immobilization process. Firstly, BSA molecules are modified on silk fibers via hydrophobic force to render the surface positively charged. Then negatively charged GO nanosheets are adsorbed on the fiber surface via electrostatic interaction. In this procedure positive charges on the fiber surface are neutralized and the surface may be negatively charged due to the coverage of GO. The attached GO may repel the free GO sheets in the suspension from the silk fiber, hindering their further adsorption. This is why the simple extension of GO immersion time cannot greatly enhance the electrical conductivity (Fig. S8D). After hydrazine reduction, the chemical groups on silk-attached GO sheets are removed and the surface charge changes from negative to neutral. The free GO in the suspension can be adsorbed on the reduced GO nanosheets via π-π interactions and hydrophobic force in the next immersion step. Thus, with the repeating of coating and reduction, the silk surface coverage of graphene is significantly improved. Moreover, the GO nanosheets overlap with each other on the silk, shortening the electron transfer pathways. Therefore, the increase of surface coverage and overlap of graphene nanosheets may contribute to the high conductivity of the as-prepared graphene-silk fabrics/fibers.

In summary, we have demonstrated an effective approach to preparing highly conductive graphene-coated silk fabrics, by which graphene nanosheets could be immobilized on silk textiles with overlapped bridge structures and a high surface coverage. The sheet resistance of graphene-coated silk fabrics can be 1.5 kΩ/sq and the electrical conductivity of a single graphene-coated silk fiber reaches to 3595 S/m. This facile method provides a prompt way to prepare high-quality graphene-silk electronic

fabrics/fibers. The graphene-coated silk fabrics and fibers prepared with the approach are very promising as the functional supporting matrix and conducting fabrics/wires in future wearable electronics.

This work is financially supported by National Program on Key Basic Research Project of China (973 Program) under contract No.2013CB127804 and Chongqing Key Laboratory for Advanced Materials and Technologies of Clean Energies under cstc2011pt-sy90001 (Chongqing, China), Start-up grant under SWU111071 from Southwest University (Chongqing, China) and Chongqing Science and Technology Commission under cstc2012gjhz90002 (Chongqing, China). Z. S. Lu would like to thank the supports by the Specialized Research Fund for the Doctoral Program of Higher Education (RFDP) (Grant No. 20130182120025), Chongqing Key Natural Science Foundation (cstc2012jjA1137) and Young Core Teacher Program of the Municipal Higher Educational Institution of Chongqing.

Notes and references

a Chongqing Key Laboratory for Advanced Materials & Technologies of Clean Energies, 1 Tiansheng Road, Chongqing 400715, P. R. China

b Institute for Clean Energy & Advanced Materials, Faculty of Materials and Energy, Southwest University, 1 Tiansheng Road, Chongqing 400715, P. R. China.

c Chongqing Engineering Research Center for Rapid Diagnosis of Fatal Diseases, 1 Tiansheng Road, Chongqing 400715, P. R. China. Fax: +86-23-68254969; Tel: +86-23-68254732; E-mail: zslu@swu.edu.cn

† Electronic Supplementary Information (ESI) available: [Experimental procedures and supporting results are included in ESI]. See DOI: 10.1039/b000000x

1. A. Pantelopoulos and N. G. Bourbakis, *Systems, Man, and Cybernetics, Part C: Applications and Reviews, IEEE Transactions on*, 2010, **40**, 1-12.
2. K. Cherenack and L. van Pieterson, *Journal of Applied Physics*, 2012, **112**, 091301.
3. Q. T. H. Shubhra, A. K. M. M. Alam and M. D. H. Beg, *Materials Letters*, 2011, **65**, 333-336.
4. J. Guan and G. Chen, *Journal of Applied Polymer Science*, 2013, **129**, 2335-2341.
5. B. Liang, L. Fang, Y. Hu, G. Yang, Q. Zhu and X. Ye, *Nanoscale*, 2014, **6**, 4264-4274.
6. T.-H. Luong, T.-N. Dang, O. Ngoc, T.-H. Dinh-Thuy, T.-H. Nguyen, V. Van Toi, H. Duong and H. Le Son, in *5th International Conference on Biomedical Engineering in Vietnam*, eds. V. V. Toi and T. H. Lien Phuong, Springer International Publishing, 2015, pp. 325-328.
7. K. Cherenack, C. Zysset, T. Kinkeldei, N. Munzenrieder and G. Troster, *Advanced materials*, 2010, **22**, 5178-5182.
8. M. D. Irwin, D. A. Roberson, R. I. Olivas, R. B. Wicker and E. MacDonald, *Fibers and Polymers*, 2011, **12**, 904-910.
9. I. Cucchi, A. Boschi, C. Arosio, F. Bertini, G. Freddi and M. Catellani, *Synthetic Metals*, 2009, **159**, 246-253.
10. U. Malhotra, S. Maity and A. Chatterjee, *Journal of Applied Polymer Science*, 2015, **132**, n/a-n/a.
11. I. S. Romero, M. L. Schurr, J. V. Lally, M. Z. Kotlik and A. R. Murphy, *ACS Appl Mater Interfaces*, 2013, **5**, 553-564.
12. N. Gogurla, S. P. Mondal, A. K. Sinha, A. K. Katiyar, W. Banerjee, S. C. Kundu and S. K. Ray, *Nanotechnology*, 2013, **24**, 345202.
13. B.-J. Dong and Q. Lu, *Frontiers of Materials Science*, 2014, **8**, 102-105.
14. C. Dionigi, T. Posati, V. Benfenati, A. Sagnella, A. Pistone, S. Bonetti, G. Ruani, F. Dinelli, G. Padeletti, R. Zamboni and M. Muccini, *Journal of Materials Chemistry B*, 2014, **2**, 1424.
15. S. Tsukada, H. Nakashima and K. Torimitsu, *PLoS ONE*, 2012, **7**, e33689.
16. H. Lin, S. Xu, Y.-Q. Zhang and X. Wang, *ACS Applied Materials & Interfaces*, 2014, **6**, 11341-11347.
17. V. Georgakilas, M. Otyepka, A. B. Bourlinos, V. Chandra, N. Kim, K. C. Kemp, P. Hobza, R. Zboril and K. S. Kim, *Chemical reviews*, 2012, **112**, 6156-6214.
18. J. Liu, S. Fu, B. Yuan, Y. Li and Z. Deng, *Journal of the American Chemical Society*, 2010, **132**, 7279-7281.
19. A. C. Ferrari, J. C. Meyer, V. Scardaci, C. Casiraghi, M. Lazzeri, F. Mauri, S. Piscanec, D. Jiang, K. S. Novoselov, S. Roth and A. K. Geim, *Physical Review Letters*, 2006, **97**.
20. Y. Xia and L. Yun, *Composites Science and Technology*, 2008, **68**, 1471-1479.